STM JOURNALS

Journal of
Polymer & Composites

ISSN: 2321-2810 (Online)
ISSN: 2321-8525 (Print)
Volume 13, Special Issue 2, 2025
DOI (Journal): 10.37591/JoPC

https://journals.stmjournals.com/jopc

Research JoPC

Quasi-Dimensional Thermodynamic Performance and Emission Modelling for Dual-Fuel SI Engine Operation Using Waste-Based Producer Gas and Methane

Priyaranjan Jena[1,*], Jeewan Vachan Tirkey[2], Reetu Raj[3], Lawalesh Kumar Prajapati[4]

Abstract

Rising energy crisis and urgent need for better waste-handling techniques have gained significant attention. Integration of wastes-to-wealth and Green Energy evolution techniques are prime sustainable measures towards countering this menace. Moreover, Internal Combustion (IC) engines are significant energy consumers and their emissions play a major factor in global warming and ecological obliteration. Concerning these aspects, investigations should strive at emissions minimization and reutilization of low-impact industrial byproducts. Thus, using methane or propane for fueling IC engines when blended with greener alternate fuels like Producer gas (PG), formed of waste gasification techniques, could be very beneficial. Therefore, this study applies the inexpensive investigation approach of numerical modelling for the analysis of SI engine performance when operating on blended fuel compositions of methane and Sewage sludge-based producer gas (SSPG). The simulation is attuned with parametric conditions of 11 CR and stoichiometric Equivalence ratio (ER=1). As PG inherits lower flame-speed and calorific value (CV) than conventional fuels, varying start-of-ignition (SOI) timings and methane blends were respectively considered as the independent input parameters. The prediction accuracy of the simulation is first validated and then the potential parametric emission and performance responses were examined for favorableness. Results exposed that the engine performance and emissions are more favorable for operative SOI at around 35⁰ to 40⁰ spark advance (BTDC) and low PG-blending. ITE and IMEP maximize to 37.2% and 6.7(kW), whereas minimum attained BSFC, and CO, NO emissions are 0.304(kg/kWh), 0.58(v%) and 1095.9(ppm) respectively.

Keywords: Producer gas, thermodynamic modelling, sewage sludge, waste to energy, methane blend, SI engine simulation

INTRODUCTION

Due to rapid industrialization and the need for sustainable growth, the search for alternative fuels seeks prompt attention. On the other hand, increasing urban population results in massive amounts of municipal sewage and wastewater generation. This causes unsustainability issues. The largest annual production of sewage sludge is estimated at nearly 13.5 million tons of Dry Matter (mtDM) from the EU and 12.56 mtDM from the USA [1]. Refuse-derived fuel (RDF), combustion /incineration, pyrolysis, and gasification are the possible solutions to reusing sewage sludge [2, 3]. However, gasification is a very feasible solution among the available options, as it can solve the issues of incineration, such as SO_X emissions, heavy metal fly ash, and chlorinated dibenzodioxins and dibenzofurans generation.

***Author for Correspondence**
Priyaranjan Jena

[1,3,4]Ph.D., Department of Mechanical Engineering, Indian Institute of Technology (B.H.U.) Varanasi, Uttar Pradesh, India
[2] Associate Professor, Department of Mechanical Engineering, Indian Institute of Technology (B.H.U.), Varanasi, Uttar Pradesh, India

Received Date: March 21, 2024
Accepted Date: September 12, 2024
Published Date: February 15, 2025

Citation: Priyaranjan Jena, Jeewan Vachan Tirkey, Reetu Raj, Lawalesh Kumar Prajapati. Quasi-Dimensional Thermodynamic Performance and Emission Modelling for Dual-Fuel SI Engine Operation Using Waste-Based Producer Gas and Methane. Journal of Polymer & Composites. 2025; 13(Special Issue 2): S446–S458p.

Sewage sludge (SS) is subjected to sequences of complex chemical and physical treatments through the thermochemical processes and partial oxidation during gasification. These treatments occur at temperatures ranging between 650 and 900 °C. Gasification yield from the SS is higher once the sludge is dried to over 90% dry in solid content [2, 4]. Additionally, it is more effective and cost-efficient to use fuel derived from sewage sludge gas in IC Engine applications, as it has a higher calorific value, as opposed to further converting synthetic natural gas, di-methyl-ether, or adopting synthetic gasoline that is based on Fischer-Tropsch processing [5].

According to a majority of the research works [6, 7]. producer gas has a lower calorific value and lower flammability limit. Therefore, its application in fueling IC engines results in featuring lesser braking power, more brake-specific fuel, and unstable combustion. In order to improve the performance of SI engines, SSPG must be blended with a greater calorific value component. Methane is a viable choice, according to Szwaja et al. [5, 8]. It is because-

- Methane has a greater calorific value (35.4 MJ/Nm3)
- Methane is available widely, with Natural gas as the main resources
- Methane retains a high H/C ratio. This accounts for low CO_2-emissions
- Methane possesses superior octane number (about 120-130). It enables high compression ratio engine run and consequently enhances thermal efficiency for the process [9, 10].

The thermal efficiency can be increased using the supplementation of flame speed, or a flexible ignition system through advanced spark timings. However, the advancement is rather constrained by the unstable combustion of more blended fuels, which tend to slow down flame speed [11]. Therefore, it is necessary to study the power output from the SSPG-methane blend-powered SI engine, in terms of variations in spark advance as well as blend quality [12]. Pertaining to these research gaps in studying the simultaneous effects of variations in producer gas blend fraction (SSPG) and spark advance (SOI) on engine responses, these two parameters are the selected input parameters in this simulation study.

From many related works of literature [12, 13]. it is clear that the engine performance and combustion efficiency are significantly impacted by spark advance for a given methane-gasoline blending. Additionally, thermodynamic simulation models are powerful techniques that requires little financial investment and might be useful to address the aforementioned problems and difficulties [6]. According to Mehra et al [14]. consideration of a two-zone model (burned and unburned) integrated to quasi-dimensional modelling (QDM) could enable to execute outcomes more precisely. QD combustion models have already been verified with experimental data [14]. and could potentially model combustion in SI engines. Therefore, looking at the research gaps in brief, QDM has been applied in this work to forecast the in-cylinder pressure history, and the computed outcomes of engine power, fuel consumption, efficiency, and emissions concentrations at exhaust for the fixed modelling constrain of 1500 rpm engine run. Additionally, the impacts of simultaneously varying inputs are analyzed, verified and discussed upon in this study regarding the Peak pressure magnitude, attainment position, Indicated mean effected pressure (IMEP), Indicated thermal efficiency (ITE), Brake specific fuel consumption (BSFC), and carbon monoxide (CO), nitrogen monoxide (NO) emissions.

Pertaining to the aforementioned research gaps and operational brief, the present investigative work aims to attain the subsequent research objectives:

- Using QD thermodynamic model to effectively simulate and validate the performance of an engine powered by an SSPG-Methane combination.
- Evaluate the effect of Methane-SSPG blend and spark timing on engine performance (power, efficiency, fuel consumption, and emissions).
- Assess input factors that significantly determine SI Engine's cumulative performance.

Furthermore, this study will provide an appropriate platform for scholars and enterprises to conduct additional research and development in this field of effective and cost-efficient waste to energy conversion perspective.

NUMERICAL METHODOLOGY

When examining open and closed systems in internal combustion engines, the closed systems are represented by the power cycle, that accounts for the most important section for analyzing an engine's performance characteristics. Figure 1 illustrates the schematic approach to quasi-dimensional thermodynamic modelling (QDTM). Mathematical modelling for the developed QD-based model has been numerically programmed using the FORTRAN script. The power cycle phase of the engine thermodynamic cycle begins with the completion of Inlet valve close (IVC). Herein, the premixed reactants' composition (Air+Methane+SSPG) are considered to be homogeneous in mixture temperature, and pressure. Though the combustion process begins with spark, it incepts to lay thermodynamic influence on temperature and pressure on the mixture only when the volume of the flame kernel surpasses 0.001 times the entire in-cylinder volume [15, 16]. Subsequent to this, the combustion is presumed to spread spherically by pertaining a turbulent flame speed and separating the combustion chamber into two zones through an infinitesimal flame front thickness. The zone next to the spark is called the 'burned zone'. It entails of the combustion products. The zone, forward to the burned zone is termed as 'unburned zone', and it consists of gaseous fuel and air mixture [17].

The considered producer gas composition is 16% CO, 13% H_2, 15% CO_2 , 3% CH_4, and 53% N_2 (by volume), with a CV of around 4.5 MJ/Nm^3 [7]. Overall, the considered inputs for modeling the 4-stroked engine are (also in Figure 1):

- Geometry specifications of Engine (CR, bore dia., stroke, Valves' Diameter)
- Valve and Spark Timing (CA)
- Intake and Exhaust condition to Engine (species-P_{trap}, T_{trap})
- Charge conditions (fuel properties, equivalence ratio)
- Heat transfer coefficients

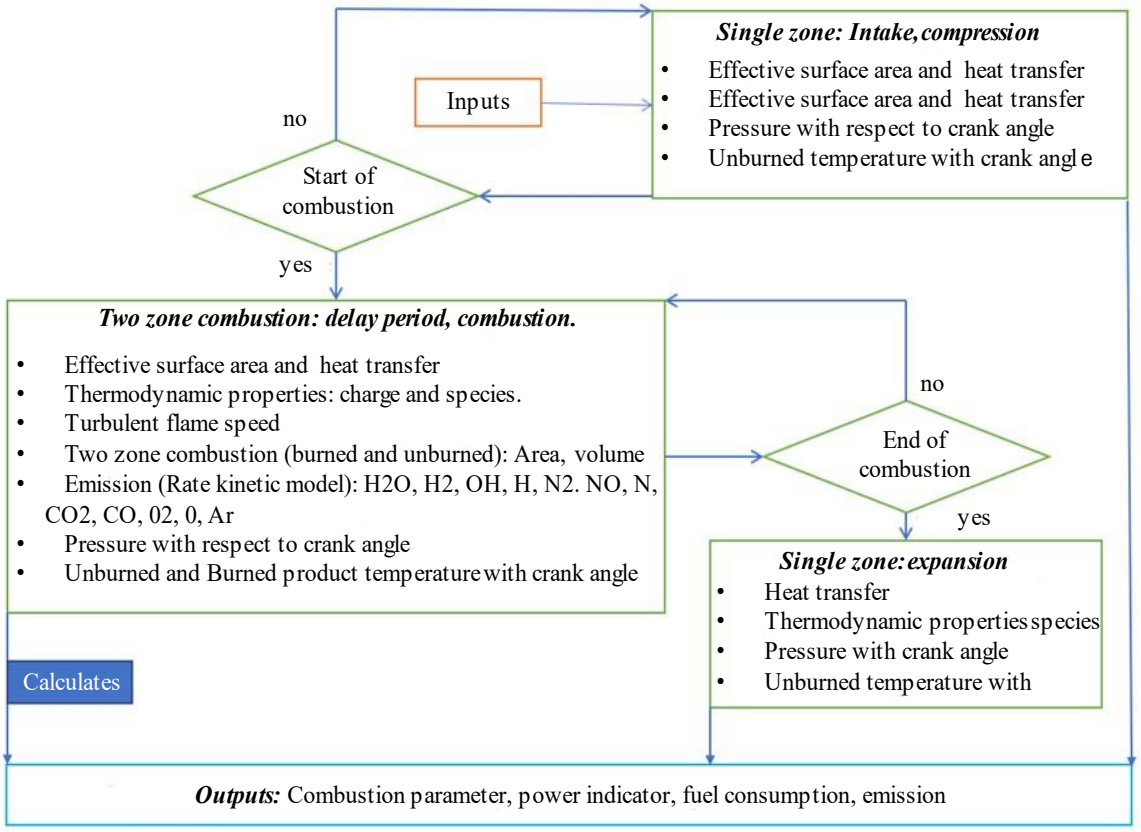

Figure 1. Layout of the engine simulation model.

Based on mass and energy conservation and from the perspective of thermodynamic state evaluation of IC Engine power cycle process, three modes of evaluation could be progressed. They are: compression (single zone), combustion (two zones), and expansion (single zone) modes [18].

Compression And Alike Single-Zone Expansion Mode Modelling

Variations in the thermodynamic pressure and temperature states in respect to the differing crank angles are governed by Eq. (1-3). Subsequently, the work done at the piston head is modelled using Eq. (4). The rate of heat transfer rate through the gas to the adjacent in-cylinder surfaces is evaluated by Annand's equation [19] (Eq. 5).

$$\frac{dp}{d\theta} = \left(\frac{1}{V}\right)\left[\left(\frac{R}{c_v}\right)\left(\frac{dQ}{d\theta}\right) - \left(\frac{Pdv}{d\theta}\right)\left(\frac{R}{c_v} + 1\right)\right] \tag{1}$$

$$\frac{dT_m}{d\theta} = T_m\left(\frac{1}{V}\frac{dV}{d\theta} + \frac{1}{P}\frac{dP}{d\theta}\right) \tag{2}$$

$$\frac{dV}{d\theta} = \frac{V_c}{2}(CR - 1)\left[(sin\,\theta) + \frac{sin\,\theta\,cos\,\theta}{\sqrt{\frac{L^2}{a_c{}^2} - sin^2\,\theta}}\right] \tag{3}$$

$$\frac{dw}{d\theta} = p\frac{dV}{d\theta} \tag{4}$$

$$\frac{q_h}{F} = \frac{aK_q}{d}(Re)^b(T_m - T_w) + c(T_m^4 - T_w^4) \tag{5}$$

Two-Zone Expansion Mode Modelling

After combustion initiation within the chamber, fundamental thermodynamic energy and mass conservation is modelled for the in-cylinder thermodynamic states through Eq. (6), where the specific heat capacity of inducted fresh air-fuel mixture and products charge (denoted as: c_{vm} and c_{vp}) are premeditated using the polynomial coefficient as depicted in Ref.-[20]. Further, the minuscule progressive variations in the induced charge volume and burned product mass are intercepted with Eq. (7,8) in respect to the differing crank angles. In this equation, A_f is the geometric flare front expanse computed applying the methods depicted in the referenced [21], u_t is turbulent flame speed and ρ is unburned charge density.

$$\left(e_p - e_m\right)\frac{dm_p}{d\theta} + m_m C_{v_m}\frac{dT_m}{d\theta} + m_m C_{v_p}\frac{dT_p}{d\theta} + p\frac{dV_{ch}}{d\theta} - \frac{dQ}{d\theta} = 0 \tag{6}$$

$$\frac{dV_{ch}}{d\theta} = \frac{dV_m}{d\theta} + \frac{dV_p}{d\theta} = \left(\frac{V_p}{m_p} - \frac{V_m}{m_m}\right)\frac{dm_p}{d\theta} + \frac{m_m R_m dT_m}{p}\frac{dT_m}{d\theta} + \frac{m_p R_p dT_p}{p}\frac{dT_p}{d\theta} - \frac{Vdp}{pd\theta} \tag{7}$$

$$\frac{dm_p}{d\theta} = -\frac{dm_p}{d\theta} = -\rho_m u_t A_f \tag{8}$$

CO and NO Species Formulations

The 12 species (H_2, H_2O, OH, N_2, H, NO, N, CO, CO_2, Ar, O, and O_2) of burned gas have been calculated by atomic balancing, and solving thirteen nonlinear equilibrium state expressions Eq. (9-15) using Newton–Raphson iterative method, as proposed by Benson et al.[15]. Moreover, the equilibrium state is governed by Eq. (16).

$$\frac{1}{2}\mathrm{H_2} \rightleftharpoons \mathrm{H} \tag{9}$$

$$\frac{1}{2}\mathrm{O_2} \rightleftharpoons \mathrm{O} \tag{10}$$

$$\frac{1}{2}\mathrm{N_2} \rightleftharpoons \mathrm{N} \tag{11}$$

$$2H_2O \rightleftharpoons 2H_2 + O_2 \quad (12)$$

$$H_2O \rightleftharpoons OH + \frac{1}{2}H_2 \quad (13)$$

$$CO_2 + H_2 \rightleftharpoons H_2O + CO \quad (14)$$

$$H_2O + \frac{1}{2}N_2 \rightleftharpoons H_2 + NO \quad (15)$$

$$(dG)_{T,p} = 0 \quad (16)$$

As the CO and NO formation during combustion have non-equilibrium behavior [20], the rate kinetic model method was espoused to simulate their concentrations. The NO modelling was simulated by means of the extended Zeldovich mechanism, which has been discussed in brief at Lavoie et al. [22]. And, the rate kinetic methodology has been pragmatic towards finding the CO concentration. Thus, it was accordingly modelled using the correlations presented in the works of Benson and Baruah [15, 23]. The model involved the fundamental reactions of Eq. (17-19). However, as the temperature falls with expansion, the CO concentration lags behind the equilibrium value.

$$CO + OH \overset{k_f(or)k_b}{\Longleftrightarrow} CO_2 + H \quad (17)$$

$$CO + O_2 \overset{k_f(or)k_b}{\Longleftrightarrow} CO_2 + O \quad (18)$$

$$\frac{1}{V}\frac{d}{dt}\left[[CO]V\right] = -k_f[CO_2][OH] + k_b[CO_2][H] \quad (19)$$

RESULTS AND DISCUSSIONS

This section initially presents a validation study for the thermodynamic simulation model. Thereafter, the analysis of various performance and emission responses is presented according to the simulated results for varying input levels.

Validation Corresponding To P-Theta Diagram

The quasi-dimensional (QD) simulation outcomes have been validated from the sole available experimental report on SI IC engine performance when fueled with SSPG and CH_4 blends, which is Szwaja et al. (ref.-[5]). Towards maintaining consistency in the validation, modelling specifications for the QDTM are set identically with the engine specifications mentioned in the referred experimentation. These engine specifications are tabulated in Table 1 and have also been implemented for discussions on the modelled performance and emission outcomes and its respective analysis in the following sections. As this study inspected QD modelling of single-cylinder engine performance outcomes, whereas the experimentation considered a four-cylinder SI engine, the experimental performance outcomes were reduced particular to the single-cylinder-based engine operation. Figure 2 depicts the simultaneous traces of both simulation and experimental in-cylinder pressure with respect to the crank-angle variations. Regarding variation of the in-cylinder pressure, the QD-based simulation outcomes are found to be closely in match with the traces of corresponding experimental in-cylinder pressure respective to the crank-angle variations. The maximum deviation in in-cylinder pressure with regards to any crank-angle position was within the 7% deviation, also depicted in Fig. 2. Although the peak pressure nearly matched with regards to the crank-angle position, the pressure tracing showed relatively a larger amount of deviation in crank position during the early compression phase. It must be noted that a decline in the actual reduced temperature and pressure at the early compression phase, could possibly result in the small deviations between the experimental and simulated in-cylinder pressure outcomes. Moreover, the experimental findings consisted of pressure versus crank-angle traces that are recorded over 100 consecutive cycles, and the minute observed variations may be attributed to the many cyclic oscillations that acted as noise in the examination of performance and emission patterns. Thus, the peak observed experimental traces were considered for the in-cylinder pressure validation.

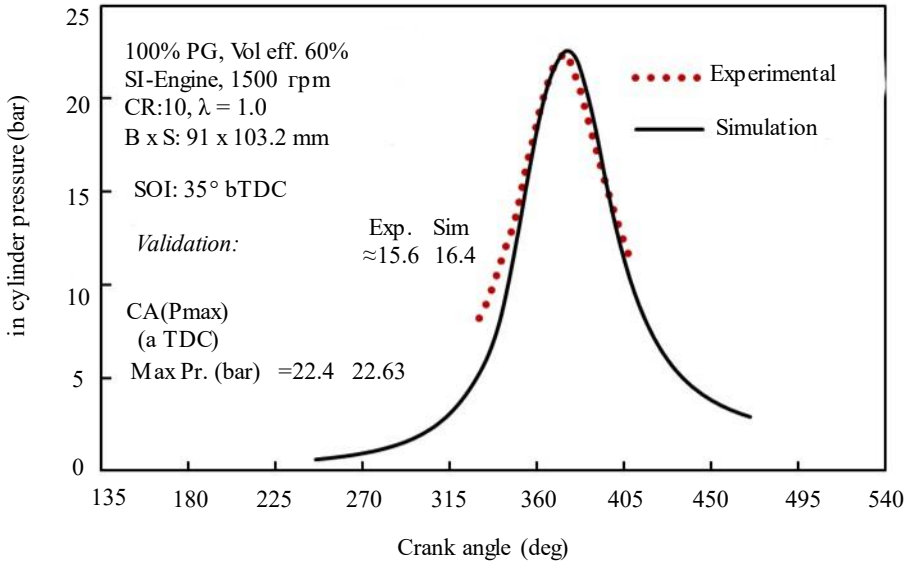

Figure 2. Validation with experimental P-Θ plot.

Table 1. Specifications of the modelled SI engine.

Engine entity	Engine specification
Engine type	4 Stroke-SI Engine
Engine model	Freely aspirated, Wiscon TM27 model [24]
Stroke (mm)	103.2
Compression ratio (r)	11:1
length of connecting rod(mm)	136.5
Set Equivalence ratio	1.0
Bore Diameter (mm)	91.0
PG fraction in volume%	10-90% *(variable)*
Start of ignition (crank angle, θ)	30-45 BTDC *(variable)*
Revolutions per minute (RPM)	1500 (maintaining 50 Hz AC frequency)

Validation Corresponding to Various Blend-Fractions

For further accessing consistency of the applied QD model with respect to blend fraction variations of PG in blended fuel intake compositions, the corresponding Brake power (BP) outcomes are also validated by referring to the same experimental study (Ref.-[5]). Fig. 3 summarizes the simulation outcomes for brake power with respect to the varying relative air-fuel ratios for the various fuel blend proportions (0.0%, 20%, 40%, and 50% SSPG blends with methane). The nature of the simulation results profile coincides extremely well with the experimental one, although it departs only slightly (on average within 5%) from what the QD model predicts for normal engine performance with fixed 30º BTDC spark timing and 11CR. When running on an SSPG and methane blend, the confirmed QD model will thus be used from onward to access these engine outputs.

The experimental trace, however, is the result of numerous cycle variations, and the program's assumed assumptions are still present in the numerical model. Since then, the operation of the SSPG-Methane blend and spark timing has been evaluated for engine performance (power, fuel consumption, and emission) using the verified quasi-dimensional model.

Abiding with the objectives, the effects of simultaneously varying inputs upon peak pressure, its CA-position, IMEP, ITE, BSFC, and emissions of CO as well as NO, is studied by using the line and radar plots developed using Microsoft EXCEL. The emerged variation trends of different output parameters are briefly reviewed with experimental kinds of literature and discussed in the following sections.

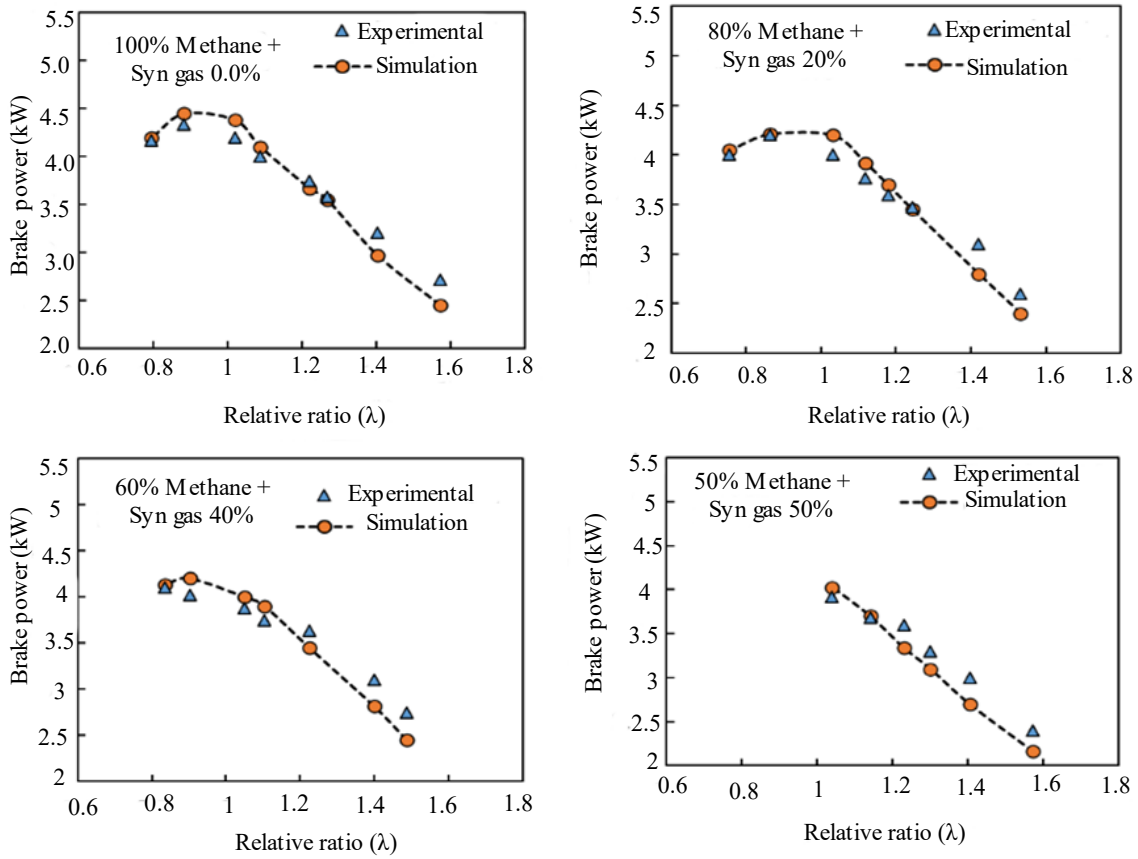

Figure 3. Validation for different blends of SSPG in methane.

Effects on Peak Pressure, and Its Position

These simultaneous plots could yield significant details regarding indicated power development, internal combustion and power conversion efficiency for various intake fuel blends with respect to advancing of spark (SOI). As seen in Figure 4, with the advancing of SOI, the crank-angle position corresponding to peak pressure also advances, pertaining to faster quenching of combustion [25, 26] and increased heat loss through Anand's correlation [27]. The peak pressure also increases with advancing SOI, as depicted in Figure 5, pertaining to more heat-release duration. Besides, with increasing SSPG-blend, the CA-duration for attaining peak pressure increases corresponding to any specific spark timing, attributing to slow flame propagation speed. Peak pressure decreases with increasing blend probably due to lower SSPG calorific value.

Effects on IMEP

IMEP indicates the obtained power at the piston head irrespective of the cylinder size. In Fig. 6, IMEP is observed to initially increase and then gradually decrease with increasing SOI. The initial increase could attribute to increasing in-cylinder temperature [28], whereas the following gradual decrease could result due to unstable combustion occurring at early spark [7, 29]. Besides, with increasing SSPG blend BMEP is observed to decrease, probably attributing to the lower calorific value of SSPG [30].

Effects on ITE

From the radar plot in Figure 7, it becomes convenient to visualize that B90-blend results in the greatest of obtained ITEs as compared to other blends for any corresponding spark timing (SOI). This effect indicates the occurrence of greater heat-to-work conversion efficiency, especially for SOI range from 35º to 40º BTDC. This could attribute to the development of suitable in-cylinder temperature and pressure conditions for more combustion and work-energy conversion efficiency [30].

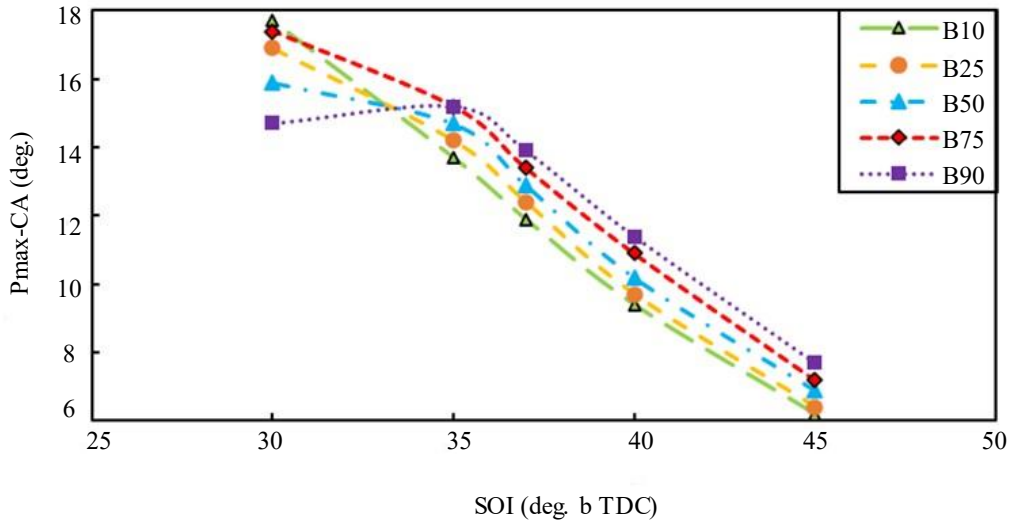

Figure 4. Simultaneous effects on crank-angle position of peak-pressure.

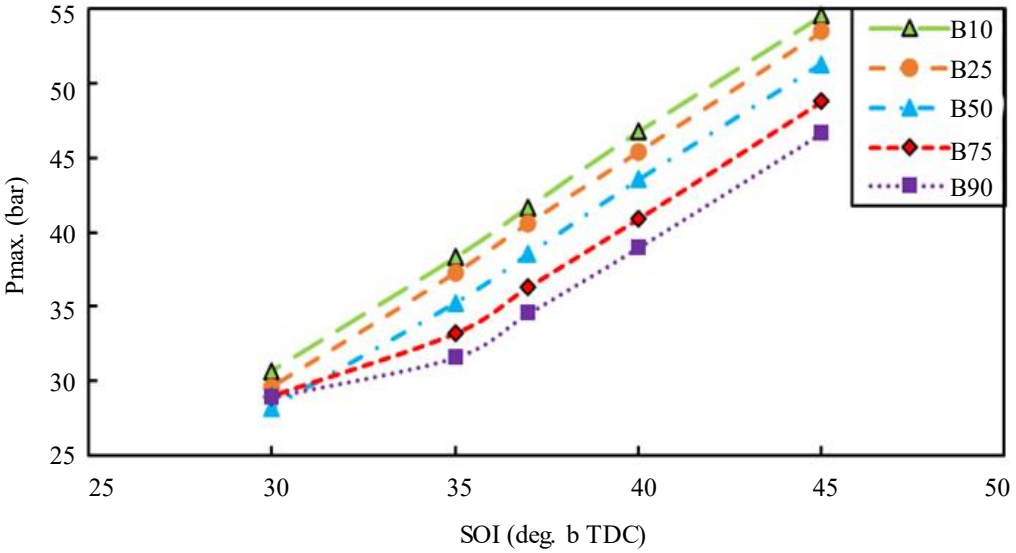

Figure 5. Simultaneous effects on modelled peak-pressure.

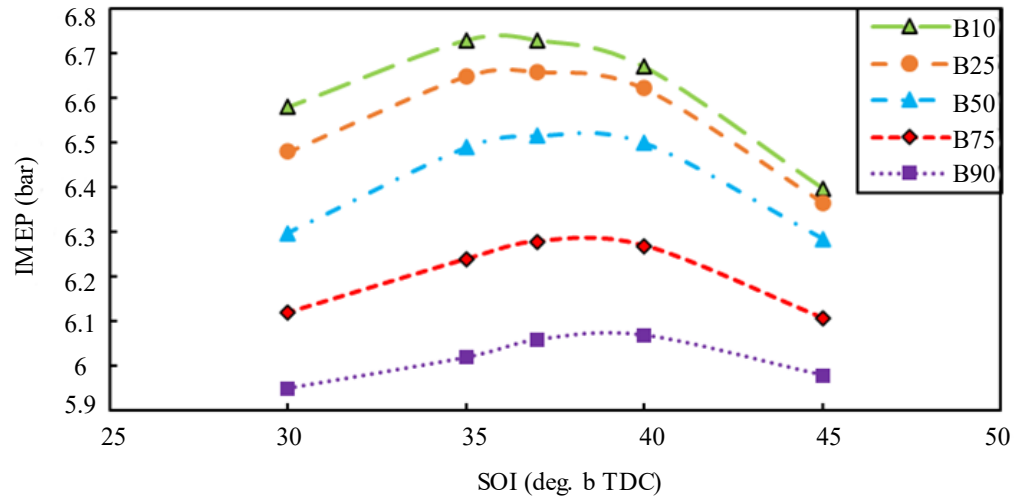

Figure 6. Simultaneous effects on IMEP.

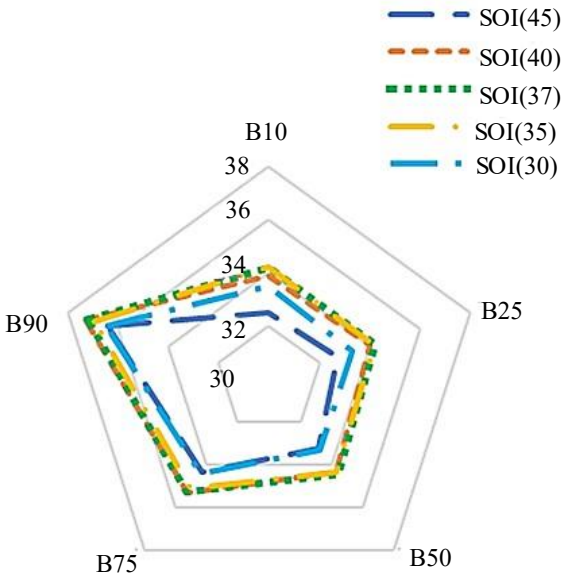

Figure 7. Simultaneous effects on ITE variations.

Effects on BSFC

BSFC represents the fraction of energy in fuel intake that is turned into output power at the engine shaft. It is the ratio of fuel intake- rate to the produced BP. From Figure 8, BSFC is observed to slightly decrease and then similarly increase corresponding to SOI increase. The pattern relates to the contrary pattern for IMEP or engine power [28]. Besides, the slightness could be due to better combustion occurring at mid-ranged SOI [30], and resulting more in fuel intake. Besides, increasing blending is seen to increase BSFC more rapidly, which could again attribute to the lower calorific value of SSPG [30]. when the shaft is set to run at a constant 1500 rpm [31].

Effects on CO-Emission

CO emission primarily represents incomplete oxidation of the hydrocarbon-based fuel. In Figure 9, CO emission is observed to increase with increasing SOI-value. As the in-cylinder temperature increases with the spark advancing [28]. the consequent oxygen demand also increases. As the intake oxygen input is stationary for the model, an oxygen scarcity builds up in the combustion chamber, probably resulting in increased CO generation. Besides, with increasing SSPG blending, CO-generation is also observed to increase, pertaining to increased CO-content in the intake charge [5].

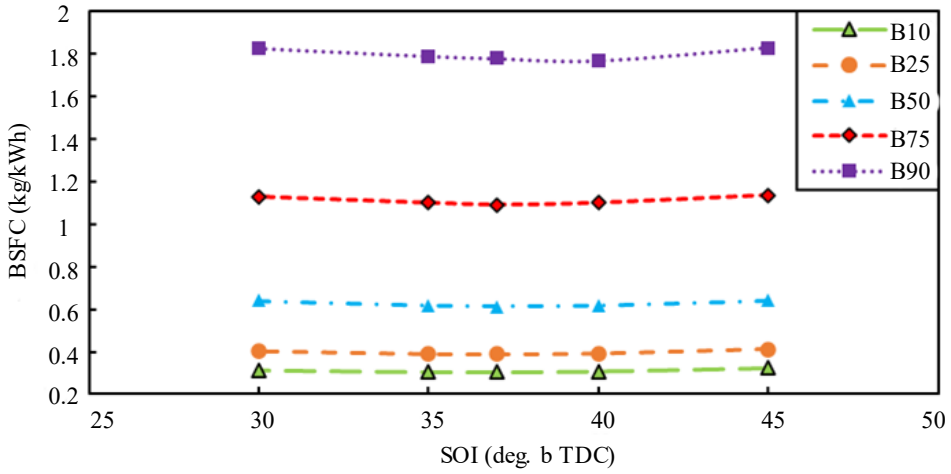

Figure 8. Simultaneous effects on BSFC variations.

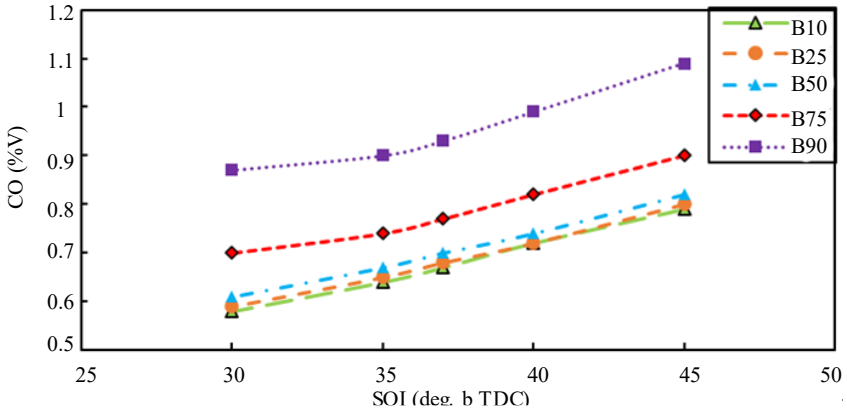

Figure 9. Simultaneous effects on CO-emission.

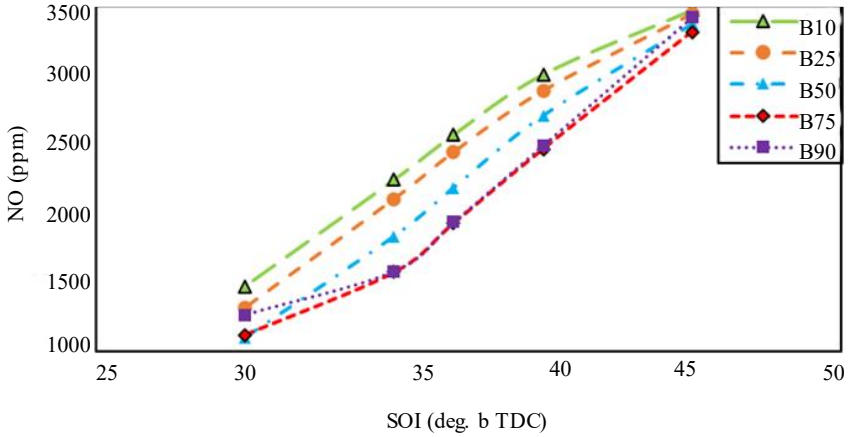

Figure 10. Simultaneous effects on NO-emission.

Effects on NO-Emission

NO-generation is governed through Zeldovich mechanism modeling for this numerical simulation, so its emission is favored by high temperature, oxygen availability and proper combustion duration [32]. From Figure 10, NO is observed to increase with SOI advance for any modeled blended fuels. This again verifies the acquirement of higher in-cylinder temperature [28] and increased oxygen demand with the advancing of SOI [33]. Further, NO-emission is observed to decrease with the increase of blending, probably attributing to decreasing heat release from increasing blend of SSPG having lower calorific value [30].

CONCLUSION

The considered performance and emission parameters of the specific SI engine fueled and operating on different blends of Sewage-sludge based Producer gas (SSPG) and methane (CH4), for the stoichiometric equivalence ratio equal to 1 and running at 1500 RPM and 11 CR, was numerically modeled using the FORTRAN-based codes. Outcome datasets from 25 model runs were reported with varying inputs of SSPG blends and SOI values. As per the model results, the varying start of ignition (SOI) and amount of SSPG blending (Blend%) lay greater impacts on the considered outputs. The simulation findings are found to be in good accord with data from diverse investigative literature.

- A validated quasi-dimensional thermodynamic model was efficaciously active towards the simulation of parametric responses of dual fuel mode spark ignition engine.
- A mid-ranged SOI (at 35º ~ 40º BTDC), highlighted better ITE, IMEP, and BSFC, whereas greater SOI resulted in increased emissions.
- Increasing SSPG-blend(>B50) although featuring better ITE, is also observed to decrease IMEP and increase CO emissions.

ABBREVIATIONS AND NOMENCLATURE

ANOVA	Analysis of Variance	Symbols	
BMEP	Brake-mean effective pressure		
BTDC	before Top Dead Center	a_c	Crank length
BP	Brake Power	α,θ	Crank angle
BR	Blend Ratio in V%	C_p	Specific heat at constant pressure
BSFC	Brake-Specific Fuel Consumption	C_v	Specific heat at constant volume
BTE	Brake Thermal Efficiency	f	Fraction (0-1)
CR	Compression Ratio	L	Connecting rod length
CA	Crank angle	ρ_u	Density of unburned charge
CD	Combustion duration (10V%-90V%)	Φ	Fuel-air equivalence ratio
CO	Carbon mono-oxide	K_{1b}	Backward rate constant
CV	Calorific value	m	Mass (kg)
ER	Equivalence ratio	K_{1f}	Forward rate constant
HHV	Higher Heating Value	p	Product
FS	Flame Speed	R	Gas constant
IT	Ignition timing	R_j	Rate constant
ITE	Indicated Thermal Efficiency	S_p	Mean piston speed
LIVC	Late Inlet-valve Closure	u'	Turbulent flame intensity
IMEP	Indicated Mean Effective Pressure	T	Turbulent nature
NO	Nitrogen Oxide	u,m	Mixture of fresh charge, unburnt
PG	Producer Gas	V%	Percentage by volume
PP	Peak pressure	V	Volume (m^3)
SOI	Start of Ignition		
SI	Spark Ignition		
SSPG	Sewage Sludge Producer Gas		
QDTM	quasi-dimensional thermodynamic modeling		

In summary, the thermodynamic-driven numerical approach predicted and demonstrated that utilizing methane and PG blends in the SI engine possibly will potentially improve performance and significantly reduce NO emissions across a range of operating conditions. Moreover, the current numerical model is expected to prove valuable for forthcoming thermodynamic and experimental investigations into SI engines when powered by alternative fuels.

Declaration of Interest

The authors declare that they have no known financial interests or personal relationships which could have resulted to influence the work reported in this paper. ISSN: 2278-2257 (Online), ISSN: 2348-9553 (Print)

REFERENCES

1. Kiselev A, Magaril E, Magaril R, Panepinto D, Ravina M, Zanetti MC. Towards circular economy: Evaluation of sewage sludge biogas solutions. Resources. 2019;8(2):91.
2. Samolada M, Zabaniotou A. Comparative assessment of municipal sewage sludge incineration, gasification and pyrolysis for a sustainable sludge-to-energy management in Greece. Waste management. 2014;34(2):411-20.
3. Basu P. Biomass gasification and pyrolysis: practical design and theory: Academic press; 2010.
4. Spinosa L, Ayol A, Baudez J-C, Canziani R, Jenicek P, Leonard A, et al. Sustainable and innovative solutions for sewage sludge management. Water. 2011;3(2):702-17.
5. Szwaja S, Kovacs VB, Bereczky A, Penninger A. Sewage sludge producer gas enriched with methane as a fuel to a spark ignited engine. Fuel processing technology. 2013;110:160-6.
6. Kumararaja L. Modelling equations for the properties of producer gas generated from biomass gasifiers. International Journal of Applied Mathematical Science. 2016;9:103-12.
7. Homdoung N, Tippayawong N, Dussadee N. Effect of ignition timing advance on performance of a small producer gas engine. International Journal of Applied Engineering Research. 2014;9(13):2341-8.

8. Kakaee A-H, Paykani A, Ghajar M. The influence of fuel composition on the combustion and emission characteristics of natural gas fueled engines. Renewable and Sustainable Energy Reviews. 2014;38:64-78.
9. Thurnheer T, Soltic P, Eggenschwiler PD. SI engine fuelled with gasoline, methane and methane/hydrogen blends: heat release and loss analysis. International journal of hydrogen energy. 2009;34(5):2494-503.
10. Diéguez P, Urroz J, Marcelino-Sádaba S, Pérez-Ezcurdia A, Benito-Amurrio M, Sáinz D, et al. Experimental study of the performance and emission characteristics of an adapted commercial four-cylinder spark ignition engine running on hydrogen–methane mixtures. Applied energy. 2014;113:1068-76.
11. Szybist JP, Busch S, McCormick RL, Pihl JA, Splitter DA, Ratcliff MA, et al. What fuel properties enable higher thermal efficiency in spark-ignited engines? Progress in Energy and Combustion Science. 2021;82:100876.
12. Jena P, Tirkey JV. Efficiency improvement investigation through Miller cycle strategy for SI engine operating on stoichiometric producer gas and methane blends. Thermal Science and Engineering Progress. 2024;47:102309.
13. Jena P, Tirkey JV. Power and efficiency improvement of SI engine fueled with boosted producer gas-methane blends and LIVC-miller cycle strategy: Thermodynamic and optimization studies. Energy. 2024;289:130068.
14. Mehra RK, Duan H, Juknelevičius R, Ma F, Li J. Progress in hydrogen enriched compressed natural gas (HCNG) internal combustion engines-A comprehensive review. Renewable and Sustainable Energy Reviews. 2017;80:1458-98.
15. Horlock JH, Winterbone D. The thermodynamics and gas dynamics of internal-combustion engines. Volume II. 1986.
16. Papagiannakis R, Zannis T. Thermodynamic analysis of combustion and pollutants formation in a wood-gas spark-ignited heavy-duty engine. International journal of hydrogen energy. 2013;38(28):12446-64.
17. Perini F, Paltrinieri F, Mattarelli E. A quasi-dimensional combustion model for performance and emissions of SI engines running on hydrogen–methane blends. International Journal of Hydrogen Energy. 2010;35(10):4687-701.
18. Tirkey J, Gupta H, Shukla S. Integrated gas dynamic computational modelling and thermodynamic combustion diagnostics of multicylinder four-stroke spark ignition engine using compressed natural gas as a fuel. International Journal of Sustainable Energy. 2010;29(2):59-75.
19. Thermodynamics, Group FM, Annand W. Heat transfer in the cylinders of reciprocating internal combustion engines. Proceedings of the Institution of Mechanical Engineers. 1963;177(1):973-96.
20. Heywood J. Internal Combustion Engine Fundementals. McGrawHill series in Mechanical Engineering (Vol. 21). 1988.
21. Curto-Risso P, Medina A, Hernández AC. Optimizing the geometrical parameters of a spark ignition engine: Simulation and theoretical tools. Applied Thermal Engineering. 2011;31(5):803-10.
22. Lavoie GA, Heywood JB, Keck JC. Experimental and theoretical study of nitric oxide formation in internal combustion engines. Combustion science and technology. 1970;1(4):313-26.
23. Mehrnoosh D, Asghar HA, Asghar MA. Thermodynamic model for prediction of performance and emission characteristics of SI engine fuelled by gasoline and natural gas with experimental verification. Journal of mechanical science and technology. 2012;26(7):2213-25.
24. Ma F, Wang Y, Wang M, Liu H, Wang J, Ding S, et al. Development and validation of a quasi-dimensional combustion model for SI engines fuelled by HCNG with variable hydrogen fractions. International journal of hydrogen energy. 2008;33(18):4863-75.
25. Hotta SK, Sahoo N, Mohanty K, Kulkarni V. Ignition timing and compression ratio as effective means for the improvement in the operating characteristics of a biogas fueled spark ignition engine. Renewable Energy. 2020;150:854-67.
26. Sharma M, Kaushal R. Performance and exhaust emission analysis of a variable compression ratio (VCR) dual fuel CI engine fuelled with producer gas generated from pistachio shells. Fuel. 2021;283:118924.

27. Fonseca L, Olmeda P, Novella R, Valle RM. Internal combustion engine heat transfer and wall temperature modeling: an overview. Archives of Computational Methods in Engineering. 2020;27(5):1661-79.
28. Mojaver P, Khalilarya S, Chitsaz A. Multi-objective optimization using response surface methodology and exergy analysis of a novel integrated biomass gasification, solid oxide fuel cell and high-temperature sodium heat pipe system. Applied Thermal Engineering. 2019;156:627-39.
29. Liu Q, Pachiannan T, Zhong W, Nallusamy N, Zhang Y, Li Z, et al. Effects of injection strategies coupled with gasoline-hydrogenated catalytic biodiesel blends on combustion and emission characteristics in GCI engine under low loads. Fuel. 2022;317:123490.
30. Tirkey JV, Singh DK. Thermodynamic performance and emission prediction of CI engine fueled with diesel and Vachellia nilotica (Babul) biomass-based producer gas and optimization using RSM. Petroleum Science and Technology. 2022;40(9):1084-108.
31. Tirkey J. Simulation-based investigation of producer gas and propane blended SI engine for power generation application. International Journal of Sustainable Energy. 2021;40(4):344-63.
32. Jena P, Tirkey JV, Raj R, Prajapati LK. Effect of Propane blending with Grape wood Producer gas on SI Engine performance and optimization. Applied Thermal Engineering. 2024:122480.
33. Jena P, Raj R, Tirkey JV, Kumar A. Experimental analysis and optimization of CI engine performance using waste plastic oil and diesel fuel blends. Journal of the Energy Institute. 2023;109:101286

